Hindawi
Journal of Applied Mathematics
Volume 2021, Article ID 1880822, 17 pages
https://doi.org/10.1155/2021/1880822

Research Article

Using Division Method to Convert the K-Input MIMO System to SISOs System Combined with Optimal Algorithm Application to Control of a Flexible Link System for the Oscillation (K=1,2)

Nguyen Cong Danh

The Independent Researcher, Phnom Penh, Cambodia

Correspondence should be addressed to Nguyen Cong Danh; congdanh.ptithcm@gmail.com

Received 15 June 2021; Revised 29 June 2021; Accepted 6 August 2021; Published 26 August 2021

Academic Editor: Chong Lin

The flexible link system (FLS) was a highly nonlinear model, multivariable and absolutely unstable dynamic system. In practice, it is common to integrate multiple subsystems into the main system with dynamically turned k-input signals (k = 1, 2,…, N) to diversity the functionality of the main system. The flexibility of the division method to convert k-input MIMO system to SISOs system combined with the optimal algorithm creates a powerful tool that can be applied to many different MIMO nonlinear systems with high success rates. The optimal controllers can be created in the future for the flexible system is implemented on an experiment system using Arduino UNO micro-controller KIT. This paper describes division method to convert the k-input MIMO system to SISOs system, after that combined with the optimal algorithm to control for the flexible link system. Specifically, the author will conduct oscillating component analysis of a system with k input pairs (k = 1, 2) so that the author can better understand the nature of sub-components as they interact with the system.

1. Introduction

The flexible link system is a topic that attracts the attention of professionals in forming flexible structures for an automation system, from a simple model to a model with a relatively complex structure. The structural flexibility when using flexible links gives the system many advantages compared to the previous traditional model: the system volume will be less, the operation will be faster, and more flexibility, due to less system volume, the power consumption of the system is reduced. The linear quadratic optimal boundary control of the flexible robotic arm is a new proposition based on the reference of the paper [1]. I am currently researching for using this technique [1] for the other system: Ac-robot. I can apply the techniques in article [2] to flexible robotic arms. The use of techniques in this article [3] in control systems is a promising research topic. The application of distributed parameter models for the robot's mobile feet based on the reference of the article [4] is a new idea. A new proposal is the use of modern controllers for the design of systems in the paper [5]. The use of the optimal controller in [6, 7] is a new proposition. The application of the fuzzy algorithm in [8, 9] is a promising idea. Path Planning [10] of a planetary robot is an important research work for the field of astronomy. Theoretical and experimental study of DLCC [11] for a flexible link system of any model is welcome. The use of achievements [12] for a soft body is an interesting topic. Maximum Allowable Load [13] of a flexible robotic arm is a promising topic.

This article focuses on the MIMO system with k-input pairs in the flexible link system, the author can apply a modern control method: The method of using the optimal controller to control the flexible link system. The application of a novel control method with a MIMO system can be applied to many complex MIMO system models. The state-of-the-art controllers will be created in the future, which will flexibly change the oscillation characteristics. The author will compare the efficiency of the above controller for the k-input system with k = 1, 2. This can be checked to show effectiveness of the real system. Through this article, the reader can find out the effectiveness of the above control method for a system. The author will also compare the pros and cons of a system using an optimal controller versus a system without any controller. Examining sub-components in a system with k inputs (k = 1, 2) is essential for the maintenance of a system. Sub-components can have more or less impact on a system depending on how much they affect the server. This paper will give an overview through the evaluation of simulation results. From there, the author can confirm their impact on a host system. Previous studies have not been able to show the existence of components that make up a system. Besides, the operation of sub-components in a host system has not been investigated meticulously in previous studies. Sub-components here can be variables that describe an individual form of activity in the constitutive of the system's motions. Specifically in this article are the levels of flexible link properties, the degree of oscillation around the specified position,....Therefore, controlling the behavior of a sub-component in a large system is an important task. Readers can understand that the components involved in the operation of the system work in harmony with each other or not? Do they interact with each other? The answers to these questions will be presented through the analytical sections of this paper. The difference of this paper compared to other papers is the detailed description of the operation of one of the elements constituting the system with 1 input pair, 2 input pairs... These elements are very diverse in terms of their structure as well as their functions. Each system has many distinct elements. Exploring these elements gives the reader a detailed look at the functions of these categories. This can give designers more incentive to create new components to improve the quality of a system's features.

2. Related Theory

2.1. Structure of the FLS. A block diagram showing the controller based on the Arduino UNO Kit is provided in Figure 1. The FLS system consists of a flexible metal (LINK) rod attached to one end of the DC deceleration motor, the other (TIP) with an acceleration sensor to measure the horizontal oscillation. Motor rotates the metal horizontally, due to the flexible metal rod, so the TIP will vibrate a lot. A 720ppr encoder was used to measure the position of the current of the LINK is θ and the acceleration sensor measures the deflection of the angle (α) of the TIP (Figure 2). The control system uses the Arduino UNO Kit, the AVR ATMEGA328 micro-controller reads the value from the encoder, which it receives the value from the accelerometer sensor. It implements the optimal control algorithm and supplies PWM signals to the motor. The sampling frequency of the system is 4 ms.

Table 1 shows the simulation results described below.

2.2. A Mathematical Model of FLS. FLS [14, 15] can be converted into blocks for analysis, such as Figure 3.

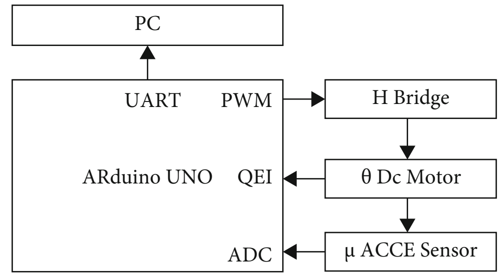

Figure 1: A block diagram of FLS control system.

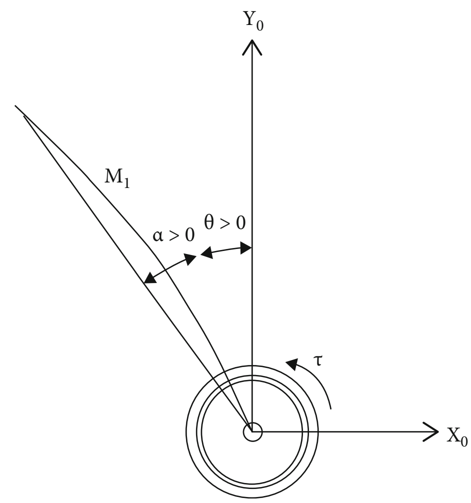

Figure 2: A Spatial model of FLS [14].

The input of the FLS system is the voltage, which supplies for (V_m) voltage to the motor, the two outputs are controlled by the position of the motor's rotation and the deviation of the angle of the LINK (Figure 3).

Using Lagrange equation to determine the equations of motion of the system through the total kinetic energy and the total potential energy of the elements in the FLS system in motion.

The potential energy of FLS system is the elastic energy when the LINK vibrates:

$$V = \frac{1}{2} K_S \alpha^2 \tag{1}$$

The kinetic energy of a FLS system consists of two components, the kinetic energy component rotated by the motor and the kinetic energy component when the LINK is deviated:

$$T = \frac{1}{2} J_{eq} \dot{\theta}^2 + \frac{1}{2} J_L \left(\dot{\theta} + \dot{\alpha} \right)^2 \tag{2}$$

Table 1: Physical specifications of the real system [14].

Symbol	Description	Value	Unit
B_{eq}	Equivalent viscous damping coefficient	0.004	Nm/(rad/s)
η_g	Gearbox efficiency	0.9	
K_t	Motor torque constant	0.0134	N-m/A
K_m	Back-emf constant	0.0134	V-s/rad
J_{eq}	Moment of inertia of the rotor of the motor	$2.08x10^{-3}$	$Kg.m^2$
R_m	Armature resistance of motor	1.9	Ω
η_m	Motor efficiency	0.8	
J_L	Equivalent moment of inertia at the LINK	0.0038	$Kg.m^2$
m	Mass of LINK	0.115	Kg
L	Length to LINK's center of mass	0.25	m
K_s	Stiffness of LINK	1.3	Nm/rad
B_L	Equivalent viscous damping coefficient of LINK	0.00004	Nm/(rad/s)

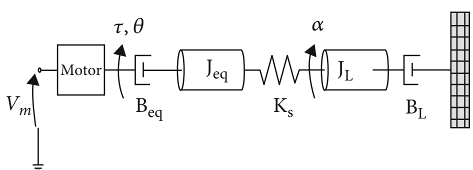

Figure 3: The Analysis of block diagram of FLS system [14].

Lagrange's the equation:

$$L = T - V = \frac{1}{2}J_{eq}\dot{\theta}^2 + \frac{1}{2}J_L\left(\dot{\theta}+\dot{\alpha}\right)^2 - \frac{1}{2}K_S\alpha^2 \tag{3}$$

The differential components of the Lagrange equation follows θ:

$$\begin{cases} \dfrac{\partial L}{\partial \dot{\theta}} = J_{eq}\dot{\theta} + J_L\left(\dot{\theta}+\dot{\alpha}\right) \\ \dfrac{d}{dt}\left(\dfrac{\partial L}{\partial \dot{\theta}}\right) = J_{eq}\ddot{\theta} + J_L\left(\ddot{\theta}+\ddot{\alpha}\right) \\ \dfrac{\partial L}{\partial \theta} = 0 \end{cases} \tag{4}$$

The differential components of the Lagrange's equation follow α:

$$\begin{cases} \dfrac{\partial L}{\partial \dot{\alpha}} = J_L\left(\dot{\theta}+\dot{\alpha}\right) \\ \dfrac{d}{dt}\left(\dfrac{\partial L}{\partial \dot{\alpha}}\right) = J_L\left(\ddot{\theta}+\ddot{\alpha}\right) \\ \dfrac{\partial L}{\partial \alpha} = -K_S\alpha \end{cases} \tag{5}$$

Force of the balance [27] of (4), (5) follows Lagrange equation:

$$\begin{cases} \left(J_{eq}+J_L\right)\ddot{\theta} + J_L\ddot{\alpha} + B_{eq}\dot{\theta} = \tau \\ J_L\ddot{\theta} + J_L\ddot{\alpha} + B_L\,\dot{\alpha}\, + K_S\alpha = 0 \\ \tau = \dfrac{\eta_g K_g \eta_m K_t\left(V_m - K_g K_m\dot{\theta}\right)}{R_m} \end{cases} \tag{6}$$

The ($B_{L)}$ the damping coefficient of the LINK is very small, which it can be considered as a ~0, the system of equations (6) becomes:

$$\begin{cases} \ddot{\theta} = -\dfrac{B_{eq}}{J_{eq}}\dot{\theta} + \dfrac{K_S}{J_{eq}}\alpha - \dfrac{\eta_g K_g{}^2\eta_m K_t K_m}{J_{eq}R_m}\dot{\theta} + \dfrac{\eta_g K_g \eta_m K_t}{J_{eq}R_m}V_m \\ \ddot{\alpha} = \dfrac{B_{eq}}{J_{eq}}\dot{\theta} - K_S\left(\dfrac{1}{J_{eq}}+\dfrac{1}{J_L}\right)\alpha + \dfrac{\eta_g K_g{}^2\eta_m K_t K_m}{J_{eq}R_m}\dot{\theta} - \dfrac{\eta_g K_g \eta_m K_t}{J_{eq}R_m}V_m \end{cases} \tag{7}$$

I set the state and output variables for the FLS system (k = 1) as follows:

$$\begin{cases} x_1 = \theta, x_2 = \alpha, x_3 = \dot{\theta}, x_4 = \dot{\alpha} \\ y_1 = x_1, y_2 = x_2 \end{cases} \tag{8}$$

I combine (7) and (8) to obtain the system of state equations describing the FLS system:

$$\begin{cases} \begin{bmatrix} \dot{x}_1 \\ \dot{x}_2 \\ \dot{x}_3 \\ \dot{x}_4 \end{bmatrix} = \begin{bmatrix} 0 & 0 & 1 & 0 \\ 0 & 0 & 0 & 1 \\ 0 & \dfrac{K_s}{J_{eq}} & \dfrac{-B_{eq}R_m - \eta_g K_g^2 \eta_m K_t K_m}{J_{eq}R_m} & 0 \\ 0 & -K_s\left(\dfrac{1}{J_{eq}} + \dfrac{1}{J_L}\right) & \dfrac{B_{eq}R_m + \eta_g K_g^2 \eta_m K_t K_m}{J_{eq}R_m} & 0 \end{bmatrix} \begin{bmatrix} x_1 \\ x_2 \\ x_3 \\ x_4 \end{bmatrix} + \begin{bmatrix} 0 \\ 0 \\ \dfrac{\eta_g K_g \eta_m K_t}{J_{eq}R_m} \\ \dfrac{-\eta_g K_g \eta_m K_t}{J_{eq}R_m} \end{bmatrix} V_m \\ \begin{bmatrix} y_1 \\ y_2 \end{bmatrix} = \begin{bmatrix} 1 & 0 & 0 & 0 \\ 0 & 1 & 0 & 0 \end{bmatrix} \begin{bmatrix} x_1 \\ x_2 \end{bmatrix} \end{cases} \tag{9}$$

I replaced the physical parameters from Table 1 into equation (9), the system of state equation of the FLS system has been designed:

$$\begin{cases} \begin{bmatrix} \dot{x}_1 \\ \dot{x}_2 \\ \dot{x}_3 \\ \dot{x}_4 \end{bmatrix} = \begin{bmatrix} 0 & 0 & 1 & 0 \\ 0 & 0 & 0 & 1 \\ 0 & 623.7 & -7.2 & 0 \\ 0 & -965.3 & 7.2 & 0 \end{bmatrix} \begin{bmatrix} x_1 \\ x_2 \\ x_3 \\ x_4 \end{bmatrix} + \begin{bmatrix} 0 \\ 0 \\ 479.8 \\ -479.8 \end{bmatrix} V_m \\ \begin{bmatrix} y_1 \\ y_2 \end{bmatrix} = \begin{bmatrix} 1 & 0 & 0 & 0 \\ 0 & 1 & 0 & 0 \end{bmatrix} \begin{bmatrix} x_1 \\ x_2 \end{bmatrix} \end{cases} \tag{10}$$

The transfer function of the FLS system is:

$$G(s) = \frac{479.8s^2 + 2.196 \times 10^{-10}s + 1.639 \times 10^5}{s^4 + 7.2s^3 + 965.3s^2 + 2460s} \tag{11}$$

I set state and output variables for the FLS system with 2 input pairs (k=2) as follows:

$$\begin{cases} x_1 = \theta, x_2 = \alpha, x_3 = \dot{\theta}, x_4 = \dot{\alpha}, x_5 = \theta_1, x_6 = \alpha_1, x_7 = \dot{\theta}_1, x_8 = \dot{\alpha}_1 \\ y_1 = x_1, y_2 = x_2, y_3 = x_5, y_4 = x_6 \end{cases} \tag{12}$$

I combine (7) and (8), (12) to obtain the system of state equations describing the FLS system with 2 input pairs:

$$\begin{cases} \begin{bmatrix} \dot{x}_1 \\ \dot{x}_2 \\ \dot{x}_3 \\ \dot{x}_4 \\ \dot{x}_5 \\ \dot{x}_6 \\ \dot{x}_7 \\ \dot{x}_8 \end{bmatrix} = \begin{bmatrix} 0 & 0 & 1 & 0 & 0 & 0 & 0 & 0 \\ 0 & 0 & 0 & 1 & 0 & 0 & 0 & 0 \\ 0 & \dfrac{K_s}{J_{eq}} & \dfrac{-B_{eq}R_m - \eta_g K_g^2 \eta_m K_t K_m}{J_{eq}R_m} & 0 & 0 & 0 & 0 & 0 \\ 0 & -K_s\left(\dfrac{1}{J_{eq}} + \dfrac{1}{J_L}\right) & \dfrac{B_{eq}R_m + \eta_g K_g^2 \eta_m K_t K_m}{J_{eq}R_m} & 0 & 0 & 0 & 0 & 0 \\ 0 & 0 & 0 & 0 & 0 & 0 & 1 & 0 \\ 0 & 0 & 0 & 0 & 0 & 0 & 0 & 1 \\ 0 & 0 & 0 & 0 & 0 & \dfrac{K_s}{J_{eq}} & \dfrac{-B_{eq}R_m - \eta_g K_g^2 \eta_m K_t K_m}{J_{eq}R_m} & 0 \\ 0 & 0 & 0 & 0 & 0 & -K_s\left(\dfrac{1}{J_{eq}} + \dfrac{1}{J_L}\right) & \dfrac{B_{eq}R_m + \eta_g K_g^2 \eta_m K_t K_m}{J_{eq}R_m} & 0 \end{bmatrix} \begin{bmatrix} x_1 \\ x_2 \\ x_3 \\ x_4 \\ x_5 \\ x_6 \\ x_7 \\ x_8 \end{bmatrix} + \begin{bmatrix} 0 \\ 0 \\ \dfrac{\eta_g K_g \eta_m K_t}{J_{eq}R_m} \\ \dfrac{-\eta_g K_g \eta_m K_t}{J_{eq}R_m} \\ 0 \\ 0 \\ \dfrac{\eta_g K_g \eta_m K_t}{J_{eq}R_m} \\ \dfrac{-\eta_g K_g \eta_m K_t}{J_{eq}R_m} \end{bmatrix} V_m \\ \begin{bmatrix} y_1 \\ y_2 \\ y_3 \\ y_4 \end{bmatrix} = \begin{bmatrix} 1 & 0 & 0 & 0 & 0 & 0 & 0 & 0 \\ 0 & 1 & 0 & 0 & 0 & 0 & 0 & 0 \\ 0 & 0 & 0 & 0 & 1 & 0 & 0 & 0 \\ 0 & 0 & 0 & 0 & 0 & 1 & 0 & 0 \end{bmatrix} \begin{bmatrix} x_1 \\ x_2 \\ x_3 \\ x_4 \\ x_5 \\ x_6 \\ x_7 \\ x_8 \end{bmatrix} \end{cases} \tag{13}$$

I replaced the physical parameters from Table 1 into the equation (9), the system of state equations of the FLS system has been designed:

$$\begin{cases} \begin{bmatrix} \dot{x}_1 \\ \dot{x}_2 \\ \dot{x}_3 \\ \dot{x}_4 \\ \dot{x}_5 \\ \dot{x}_6 \\ \dot{x}_7 \\ \dot{x}_8 \end{bmatrix} = \begin{bmatrix} 0 & 0 & 1 & 0 & 0 & 0 & 0 & 0 \\ 0 & 0 & 0 & 1 & 0 & 0 & 0 & 0 \\ 0 & 623.7 & -7.2 & 0 & 0 & 0 & 0 & 0 \\ 0 & -965.3 & 7.2 & 0 & 0 & 0 & 0 & 0 \\ 0 & 0 & 0 & 0 & 0 & 0 & 1 & 0 \\ 0 & 0 & 0 & 0 & 0 & 0 & 0 & 1 \\ 0 & 0 & 0 & 0 & 0 & 623.7 & -7.2 & 0 \\ 0 & 0 & 0 & 0 & 0 & -965.3 & 7.2 & 0 \end{bmatrix} \begin{bmatrix} x_1 \\ x_2 \\ x_3 \\ x_4 \\ x_5 \\ x_6 \\ x_7 \\ x_8 \end{bmatrix} + \begin{bmatrix} 0 \\ 0 \\ 479.8 \\ -479.8 \\ 0 \\ 0 \\ 479.8 \\ -479.8 \end{bmatrix} V_m \\ \begin{bmatrix} y_1 \\ y_2 \\ y_3 \\ y_4 \end{bmatrix} = \begin{bmatrix} 1 & 0 & 0 & 0 & 0 & 0 & 0 & 0 \\ 0 & 1 & 0 & 0 & 0 & 0 & 0 & 0 \\ 0 & 0 & 0 & 0 & 1 & 0 & 0 & 0 \\ 0 & 0 & 0 & 0 & 0 & 1 & 0 & 0 \end{bmatrix} \begin{bmatrix} x_1 \\ x_2 \\ x_3 \\ x_4 \\ x_5 \\ x_6 \\ x_7 \\ x_8 \end{bmatrix} \end{cases} \quad (14)$$

The transfer function of the FLS system with 2 input pairs (k=2) is:

$$\begin{aligned} G_1(s) &= \frac{479.8s^2 + 1.613 \times 10^{-10}s + 1.639 \times 10^5}{s^4 + 7.2s^3 + 965.3s^2 + 2460s} \\ G_2(s) &= \frac{-479.8s - 2.213 \times 10^{-12}}{s^3 + 7.2s^2 + 965.3s + 2460} \\ G_3(s) &= \frac{479.8s^2 + 2.196 \times 10^{-10}s + 1.639 \times 10^5}{s^4 + 7.2s^3 + 965.3s^2 + 2460s} \\ G_4(s) &= \frac{-479.8s + 1.107 \times 10^{-12}}{s^3 + 7.2s^2 + 965.3s + 2460} \end{aligned} \quad (15)$$

2.3. Method of Splitting MIMO System into SISOs System. Obviously FLS system is multivariate, the oscillator variable is α and the LINK's position variable is θ. The control voltage which supplies the motor is V_m voltage. FLS can be separated into two SISO systems. The input of the first SISO system is θ, the output of the first SISO system is the voltage V_{m1} which it supplies to the total set. The input of the second SISOs system is α, the output of the second SISO system is V_{M2} provides to the total set. The K_{POS} and K_{OSC} coefficients are used to set priorities for the system controller. 2-inputs of the second SISO system are α, α_1, 2-outputs of the second SISO system are V_{m3}, V_{m4} provides to the total set. The MIMO system for the FLS with 1 input pair is shown in Figure 4. The MIMO system for the FLS with 2 input pairs is shown in Figure 5.

3. Designing the Optimal Controller for Fls with 1 Input Pair (K=1)

3.1. Designing the Equation of State for the Oscillation of the FLS with 1 Input Pair. The author considered the system of state equations when only the variable name was α as follows:

$$\begin{cases} \begin{bmatrix} \dot{x}_1 \\ \dot{x}_2 \\ \dot{x}_3 \\ \dot{x}_4 \end{bmatrix} = \begin{bmatrix} 0 & 0 & 1 & 0 \\ 0 & 0 & 0 & 1 \\ 0 & 623.7 & 0 & 0 \\ 0 & -965.3 & 0 & 0 \end{bmatrix} \begin{bmatrix} x_1 \\ x_2 \\ x_3 \\ x_4 \end{bmatrix} + \begin{bmatrix} 0 \\ 0 \\ 479.8052 \\ -479.8052 \end{bmatrix} V_m \\ \begin{bmatrix} y_1 \\ y_2 \end{bmatrix} = \begin{bmatrix} 1 & 0 & 0 & 0 \\ 0 & 1 & 0 & 0 \end{bmatrix} \begin{bmatrix} x_1 \\ x_2 \end{bmatrix} \end{cases} \quad (16)$$

The author applied the algorithm according to the controller design of the SISOs system for the oscillation corresponding to the MIMO system with the state equation presented above.

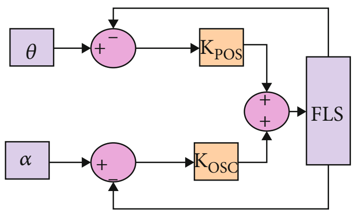

Figure 4: The diagram the optimal controller splitting MIMO into SISOs for FLS system with 1 input pairs (k=1).

3.2. Designing the Optimal Controller Splitting MIMO into SISOs for the FLS with 1 Input Pair. A control system designed in the best working mode is always in the optimal state according to a certain quality (the standard extreme value is reached).

Whether or not it is stable depends on the required quality, and understanding of the object and its impacts, based on the working condition of the control system ... In the presentation, The author designed the controller to operate in the optimal state according to the J quality criteria function as required by the problem, that traditional model without using the optimal controller has not been achieved.

The diagram of the optimal controller splitting MIMO into SISOs for the FLS is shown below (Figure 4).

$$A = \begin{bmatrix} 0 & 0 & 1 & 0 \\ 0 & 0 & 0 & 1 \\ 0 & 623.7 & -7.2 & 0 \\ 0 & -965.3 & 7.2 & 0 \end{bmatrix}; B = \begin{bmatrix} 0 \\ 0 \\ 479.8052 \\ -479.8052 \end{bmatrix}$$
$$C = \begin{bmatrix} 1 & 0 & 0 & 0 \\ 0 & 1 & 0 & 0 \end{bmatrix} \tag{17}$$

3.3. Designing the Optimal Controller for the Oscillation of FLS with 1 Input Pair. The diagram of the Optimal control for the oscillation of FLS is shown below (Figure 6).

$$A_{\alpha_1} = \begin{bmatrix} 0 & 0 & 1 & 0 \\ 0 & 0 & 0 & 1 \\ 0 & 623.7 & 0 & 0 \\ 0 & -965.3 & 0 & 0 \end{bmatrix}; B_{\alpha_1} = \begin{bmatrix} 0 \\ 0 \\ 479.8 \\ -479.8 \end{bmatrix}$$
$$C_{\alpha_1} = \begin{bmatrix} 1 & 0 & 0 & 0 \\ 0 & 1 & 0 & 0 \end{bmatrix} \tag{18}$$

The transfer function $G_{\alpha_1}(s)$:

$$G^1_{\alpha_1}(s) = \frac{479.8s^2 + 1.79 \times 10^{-11}s + 1.639 \times 10^5}{s^4 + 965.3s^2}$$
$$G^2_{\alpha_1}(s) = \frac{-479.8}{s^2 + 965.3} \tag{19}$$

The author consider the system to have the external impact $(u \neq 0)$:

$$\dot{x} = A_{\alpha_1}x + B_{\alpha_1}u \tag{20}$$

The author need to find the matrix K_{α_1} of the optimal control vector: $u(t) = -K_{\alpha_1} * x(t)$ satisfy the quality index value of J_{α_1} and J_{α_1} must reach the minimum value:

$$J_{\alpha_1} = \int_0^\infty \left(x^T Q_{\alpha_1} x + u^T R_{\alpha_1} u\right) dt \tag{21}$$

where Q_{α_1} is a positive deterministic matrix, R_{α_1} is a positive deterministic matrix.

The matrix of K_{α_1} is determined from Riccati's equation of the form:

$$K_{\alpha_1} = R_{\alpha_1}{}^{-1} B_{\alpha_1}{}^T P \tag{22}$$

The state feedback control structure is shown below (Figure 7).

Thus, the optimal control law for an optimal control problem with the quality criteria is a linear equation and it has the form:

$$u(t) = -K_{\alpha_1}(t) = -R_{\alpha_1}{}^{-1} B_{\alpha_1}{}^T P x(t) \tag{23}$$

The value of the matrix is P, P must be satisfied the equation:

$$PA_{\alpha_1} + A_{\alpha_1}{}^T P + Q_{\alpha_1} - PB_{\alpha_1} R_{\alpha_1}{}^{-1} B_{\alpha_1}{}^T P = \dot{P} \tag{24}$$

The equation (24) is known as Riccati's equation.

The author choose the values of the matrix (Q_{α_1}) and the values of the matrix (R_{α_1}) as follows:

$$Q_{\alpha_1} = \begin{bmatrix} 1 & 0 & 0 & 0 \\ 0 & 1 & 0 & 0 \\ 0 & 0 & 1 & 0 \\ 0 & 0 & 0 & 1 \end{bmatrix}, R_{\alpha_1} = 1. \tag{25}$$

The author calculate the value of the matrix K_{α_1} through Matlab software:

$$K_{\alpha_1} = lqr\left(A_{\alpha_1}, B_{\alpha_1}, Q_{\alpha 1}, R_{\alpha_1}\right) = [1.0 \ -15.8142 \ 1.0509 \ -0.3879] \tag{26}$$

3.4. Designing the Optimal Controller for FLS with 2 -Input Pairs (Figure 5)

3.4.1. Designing the Optimal Controller for the Oscillation of FLS with 2 Input Pairs (Figure 8). The author considered the system of state equations when only the variable names were α; α_1 as follows:

$$\left\{\begin{aligned}
\begin{bmatrix}\dot{x}_1\\ \dot{x}_2\\ \dot{x}_3\\ \dot{x}_4\\ \dot{x}_5\\ \dot{x}_6\\ \dot{x}_7\\ \dot{x}_8\end{bmatrix} &= \begin{bmatrix}
0 & 0 & 1 & 0 & 0 & 0 & 0 & 0\\
0 & 0 & 0 & 1 & 0 & 0 & 0 & 0\\
0 & \frac{K_s}{J_{eq}} & 0 & 0 & 0 & 0 & 0 & 0\\
0 & -K_s\left(\frac{1}{J_{eq}}+\frac{1}{J_L}\right) & 0 & 0 & 0 & 0 & 0 & 0\\
0 & 0 & 0 & 0 & 0 & 0 & 1 & 0\\
0 & 0 & 0 & 0 & 0 & 0 & 0 & 1\\
0 & 0 & 0 & 0 & 0 & \frac{K_s}{J_{eq}} & 0 & 0\\
0 & 0 & 0 & 0 & 0 & -K_s\left(\frac{1}{J_{eq}}+\frac{1}{J_L}\right) & 0 & 0
\end{bmatrix}\begin{bmatrix}x_1\\ x_2\\ x_3\\ x_4\\ x_5\\ x_6\\ x_7\\ x_8\end{bmatrix} + \begin{bmatrix}0\\ 0\\ \frac{\eta_g K_g \eta_m K_t}{J_{eq}R_m}\\ \frac{-\eta_g K_g \eta_m K_t}{J_{eq}R_m}\\ 0\\ 0\\ \frac{\eta_g K_g \eta_m K_t}{J_{eq}R_m}\\ \frac{-\eta_g K_g \eta_m K_t}{J_{eq}R_m}\end{bmatrix} V_m\\
\begin{bmatrix}y_1\\ y_2\\ y_3\\ y_4\end{bmatrix} &= \begin{bmatrix}
1 & 0 & 0 & 0 & 0 & 0 & 0 & 0\\
0 & 1 & 0 & 0 & 0 & 0 & 0 & 0\\
0 & 0 & 0 & 0 & 1 & 0 & 0 & 0\\
0 & 0 & 0 & 0 & 0 & 1 & 0 & 0
\end{bmatrix}\begin{bmatrix}x_1\\ x_2\\ x_3\\ x_4\\ x_5\\ x_6\\ x_7\\ x_8\end{bmatrix}
\end{aligned}\right.$$

$$\left\{\begin{aligned}
\begin{bmatrix}\dot{x}_1\\ \dot{x}_2\\ \dot{x}_3\\ \dot{x}_4\\ \dot{x}_5\\ \dot{x}_6\\ \dot{x}_7\\ \dot{x}_8\end{bmatrix} &= \begin{bmatrix}
0 & 0 & 1 & 0 & 0 & 0 & 0 & 0\\
0 & 0 & 0 & 1 & 0 & 0 & 0 & 0\\
0 & 623.7 & 0 & 0 & 0 & 0 & 0 & 0\\
0 & -965.3 & 0 & 0 & 0 & 0 & 0 & 0\\
0 & 0 & 0 & 0 & 0 & 0 & 1 & 0\\
0 & 0 & 0 & 0 & 0 & 0 & 0 & 1\\
0 & 0 & 0 & 0 & 0 & 623.7 & 0 & 0\\
0 & 0 & 0 & 0 & 0 & -965.3 & 0 & 0
\end{bmatrix}\begin{bmatrix}x_1\\ x_2\\ x_3\\ x_4\\ x_5\\ x_6\\ x_7\\ x_8\end{bmatrix} + \begin{bmatrix}0\\ 0\\ 479.8\\ -479.8\\ 0\\ 0\\ 479.8\\ -479.8\end{bmatrix} V_m\\
\begin{bmatrix}y_1\\ y_2\\ y_3\\ y_4\end{bmatrix} &= \begin{bmatrix}
1 & 0 & 0 & 0 & 0 & 0 & 0 & 0\\
0 & 1 & 0 & 0 & 0 & 0 & 0 & 0\\
0 & 0 & 0 & 0 & 1 & 0 & 0 & 0\\
0 & 0 & 0 & 0 & 0 & 1 & 0 & 0
\end{bmatrix}\begin{bmatrix}x_1\\ x_2\\ x_3\\ x_4\\ x_5\\ x_6\\ x_7\\ x_8\end{bmatrix}
\end{aligned}\right. \tag{27}$$

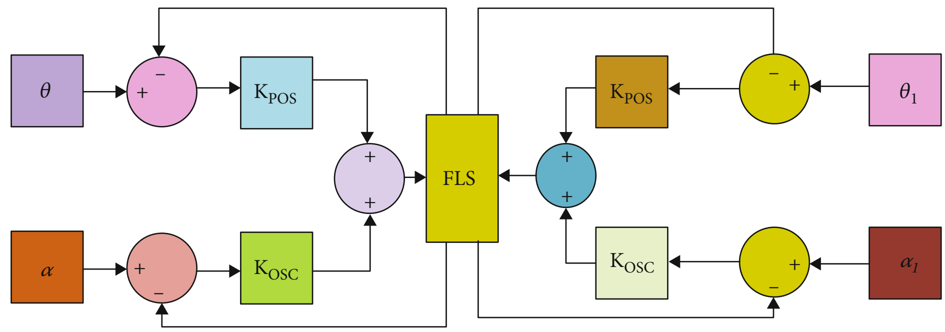

FIGURE 5: The diagram the optimal controller splitting MIMO into SISOs for FLS with 2 input pairs (k =2).

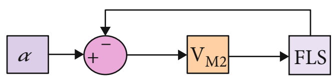

FIGURE 6: The diagram of the Optimal control for the oscillation.

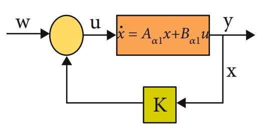

FIGURE 7: The state feedback control structure.

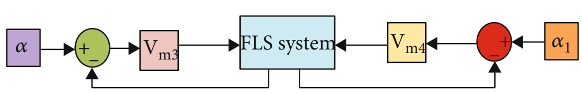

FIGURE 8: The diagram of the Optimal control for the oscillation.

The author applied the algorithm according to the controller design of the SISOs system for the oscillation corresponding to the MIMO system with the state equation presented above.

The transfer function $G_{\alpha_2}(s)$:

$$G_{\alpha_2}(s) = \frac{479.8s^2 + 1.79 \times 10^{-11}s + 1.639 \times 10^5}{s^4 + 965.3 \times s^2}$$

$$A_{\alpha_2} = \begin{bmatrix} 0 & -30.17 & 0 & 0 \\ 32 & 0 & 0 & 0 \\ 0 & 1 & 0 & 0 \\ 0 & 0 & 1 & 0 \end{bmatrix}; B_{\alpha_2} = \begin{bmatrix} 64 \\ 0 \\ 0 \\ 0 \end{bmatrix};$$

$$C_{\alpha_2} = \begin{bmatrix} 0 & 0.2343 & 2.913 \times 10^{-15} & 80.03 \end{bmatrix} \quad (28)$$

The author consider the system to have the external impact $(u \neq 0)$:

$$\dot{x} = A_{\alpha_2}x + B_{\alpha_2}u \quad (29)$$

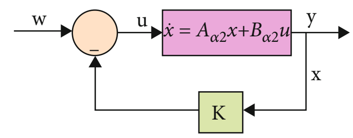

FIGURE 9: The state feedback control structure.

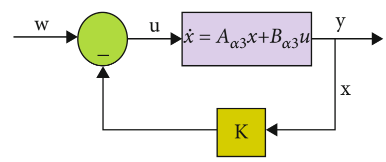

FIGURE 10: The state feedback control structure.

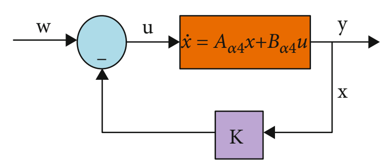

FIGURE 11: The state feedback control structure.

I need to find the matrix K_{α_2} of the optimal control vector: $u(t) = -K_{\alpha_2} * x(t)$ satisfy the quality index value of J_{α_2} and J_{α_2} must reach the minimum value:

$$J_{\alpha_2} = \int_0^{\infty} \left(x^T Q_{\alpha_2} x + u^T R_{\alpha_2} u\right) dt \quad (30)$$

where Q_{α_2} is a positive deterministic matrix, R_{α_2} is a positive deterministic matrix.

The matrix of K_{α_2} is determined from Riccati's equation of the form:

$$K_{\alpha_2} = R_{\alpha_2}^{-1} B_{\alpha_2}^{T} P \quad (31)$$

The state feedback control structure is shown below (Figure 9).

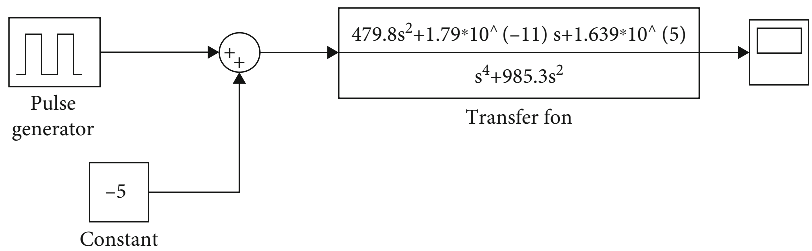

FIGURE 12: The model without using any algorithms $G^1_{\alpha_1}(s)$.

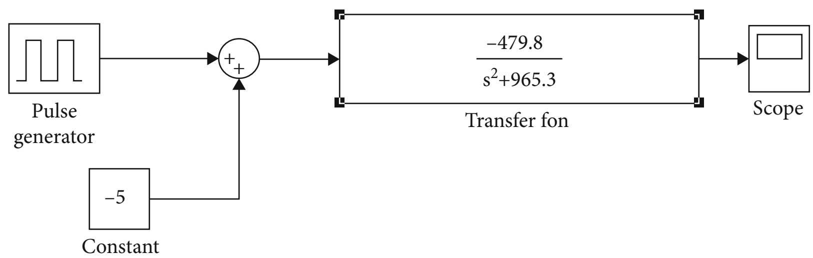

FIGURE 13: The model without using any algorithms $G^2_{\alpha_1}(s)$.

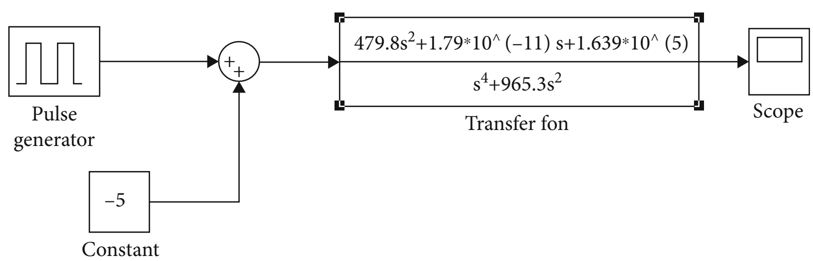

FIGURE 14: The model without using any algorithms $G_{\alpha_2}(s)$.

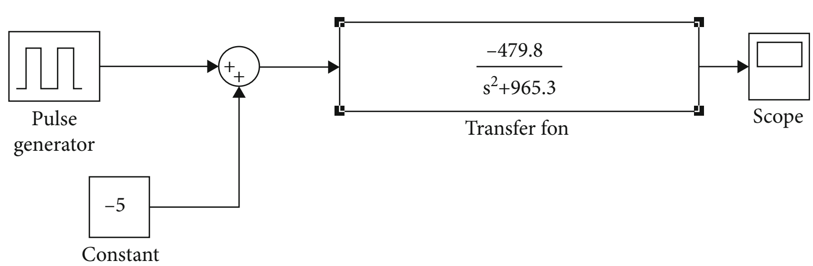

FIGURE 15: The model without using any algorithms $G_{\alpha_3}(s)$.

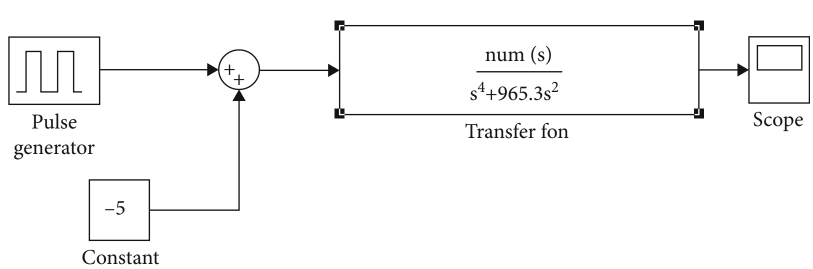

FIGURE 16: The model without using any algorithms $G_{\alpha_4}(s)$.

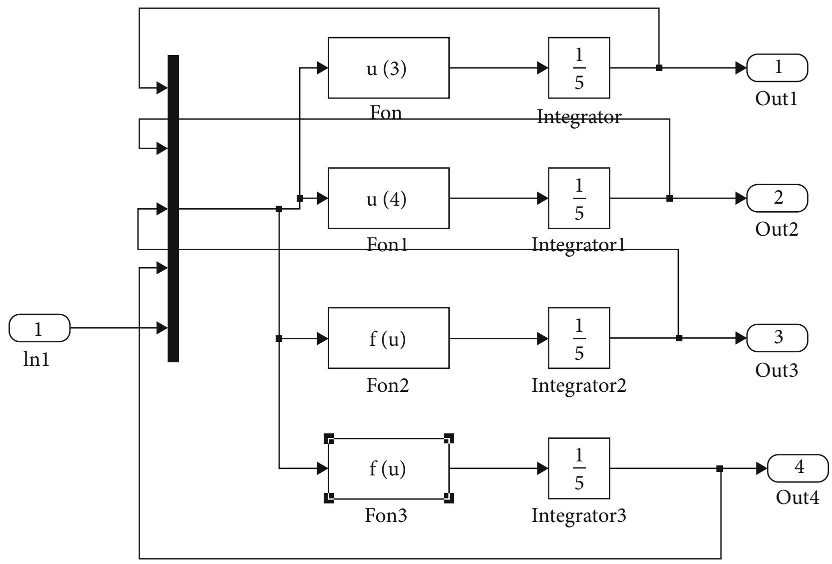

Figure 17: Applying the optimal LQR control method for the system $G_{\alpha_1}(s)$.

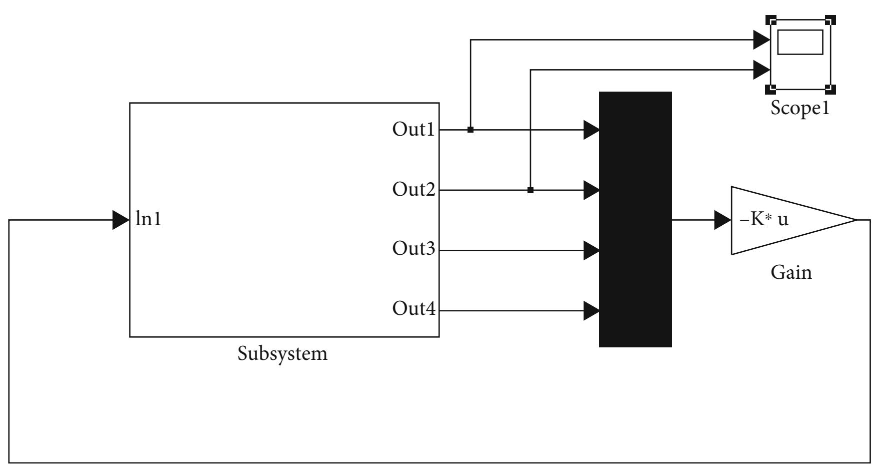

Figure 18: The system with the optimal controller $G_{\alpha_1}(s)$.

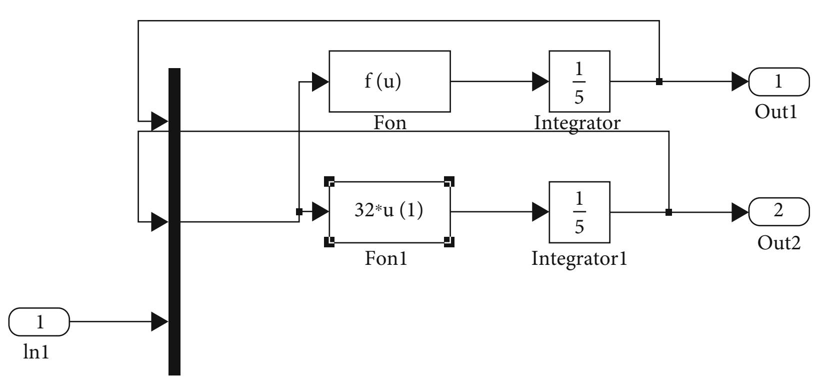

Figure 19: Applying the optimal LQR control method for the system $G_{\alpha_3}(s)$.

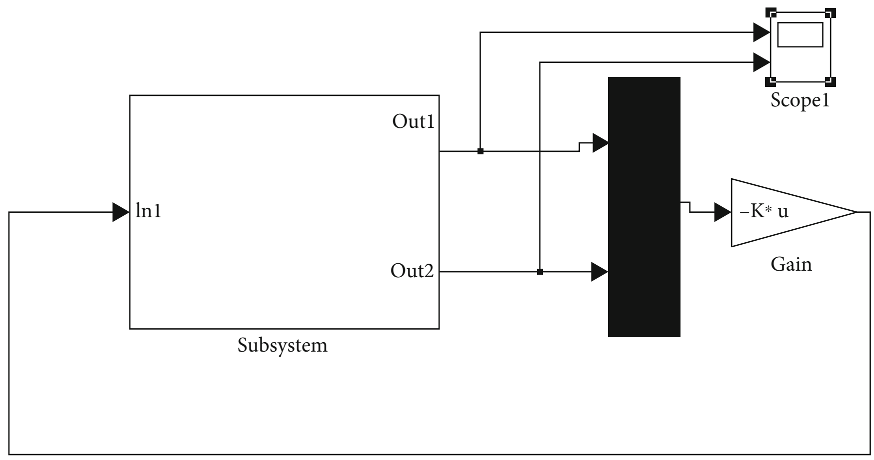

Figure 20: The system with the optimal controller $G_{\alpha_3}(s)$.

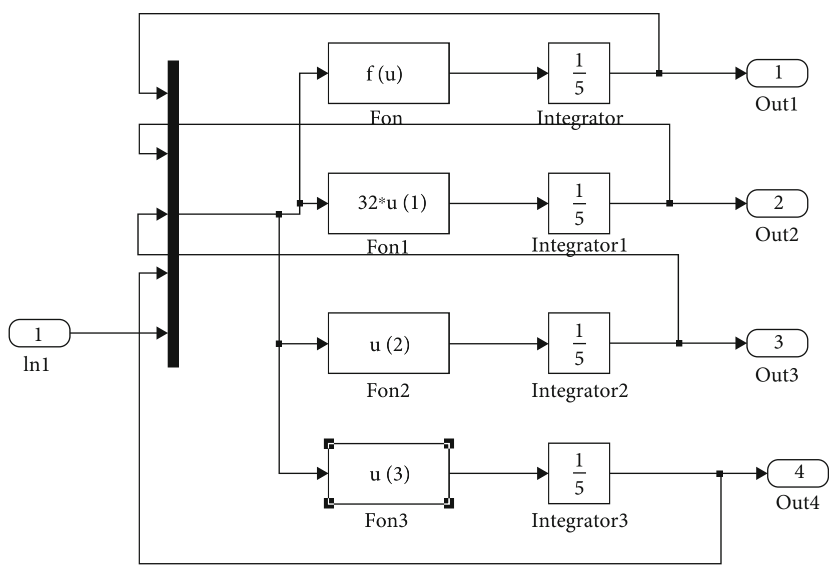

Figure 21: Applying the optimal LQR control method for the system $G_{\alpha_4}(s)$, $G_{\alpha_2}(s)$.

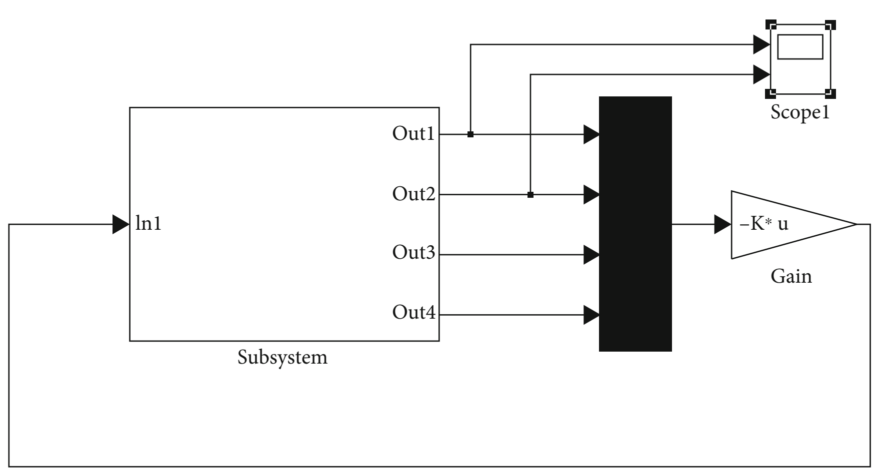

Figure 22: The system with the optimal controller $G_{\alpha_4}(s)$, $G_{\alpha_2}(s)$.

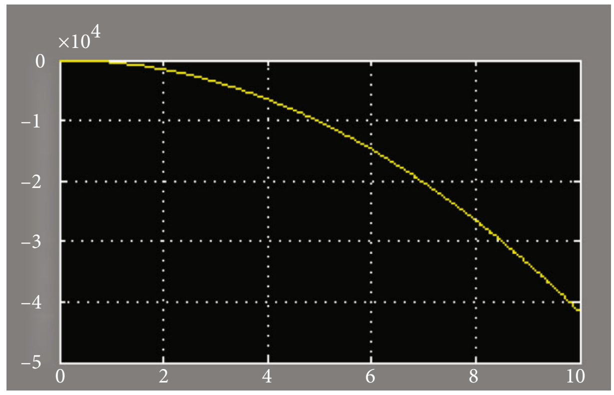

Figure 23: The simulation result without using any algorithms $G^1_{\alpha_1}(s)$.

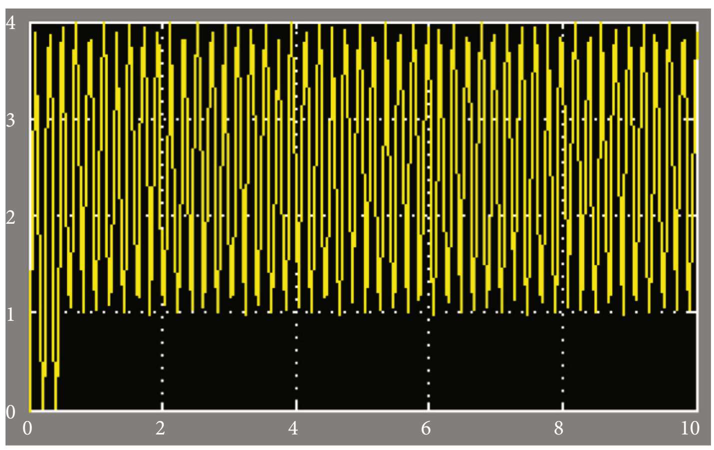

Figure 24: The simulation result without using any algorithms $G^2_{\alpha_1}(s)$.

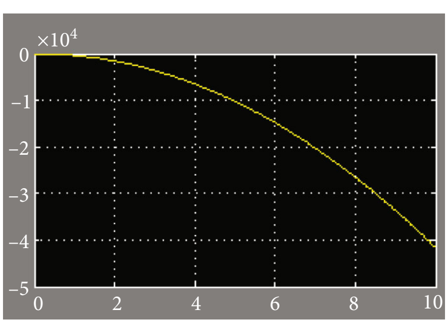

Figure 25: The simulation result without using any algorithms $G_{\alpha_2}(s)$.

Thus, the optimal control law for an optimal control problem with the quality criteria is a linear equation and it has the form:

$$u(t) = -K_{\alpha_2}(t) = -R_{\alpha_2}{}^{-1}B_{\alpha_2}{}^{T}Px(t) \tag{32}$$

The value of the matrix is P, P must be satisfied the equation:

$$PA_{\alpha_2} + A_{\alpha_2}{}^{T}P + Q_{\alpha_2} - PB_{\alpha_2}R_{\alpha_2}{}^{-1}B_{\alpha_2}{}^{T}P = \dot{P} \tag{33}$$

The equation (33) is known as Riccati's equation.

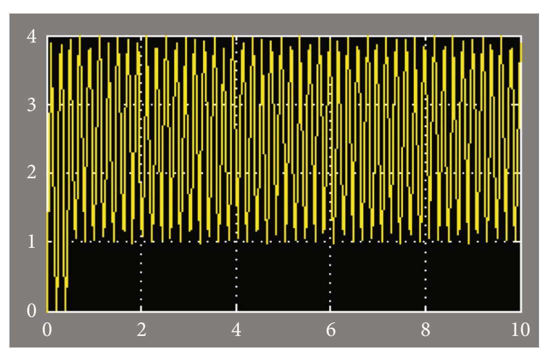

Figure 26: The simulation result without using any algorithms $G_{\alpha_3}(s)$.

The author choose the values of the matrix Q_{α_2} and the values of the matrix R_{α_2} as follows:

$$Q_{\alpha_2} = \begin{bmatrix} 1 & 0 & 0 & 0 \\ 0 & 1 & 0 & 0 \\ 0 & 0 & 1 & 0 \\ 0 & 0 & 0 & 1 \end{bmatrix}; R_{\alpha_2} = 1. \tag{34}$$

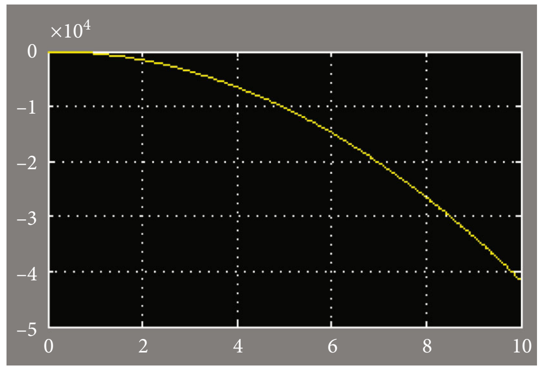

FIGURE 27: The simulation result without using any algorithms $G_{\alpha_4}(s)$.

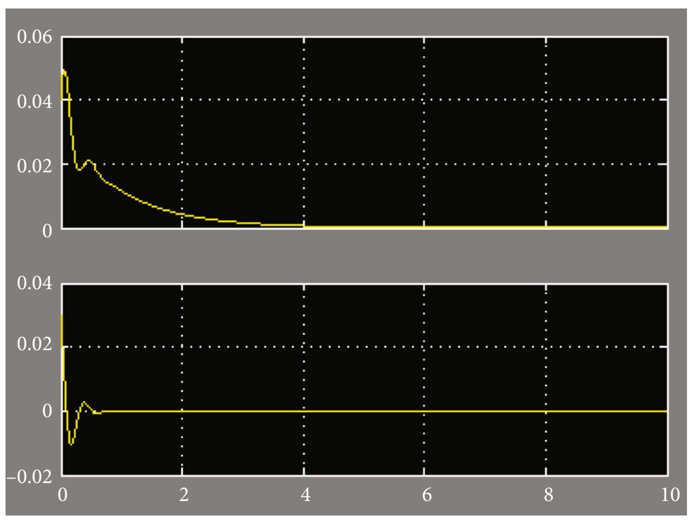

FIGURE 28: The simulation result using optimal control $G_{\alpha_1}(s)$. Initial condition: $x_1 = 0.04$, $x_2 = 0.03$, $x_3 = 0.03$, $x_4 = 0.03$.

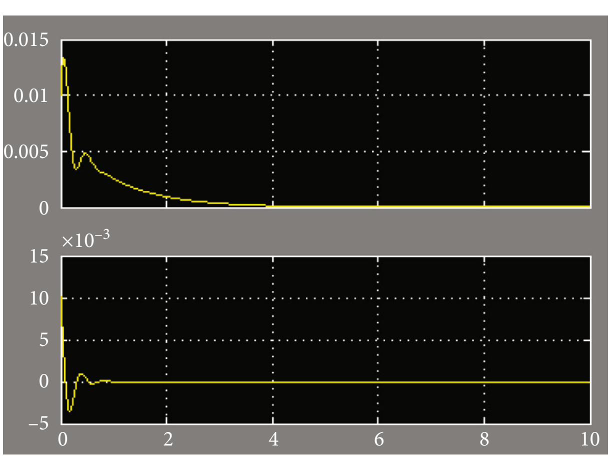

FIGURE 29: The simulation result using optimal control $G_{\alpha_1}(s)$. Initial condition: $x_1 = 0.01$, $x_2 = 0.01$, $x_3 = 0.01$, $x_4 = 0.01$.

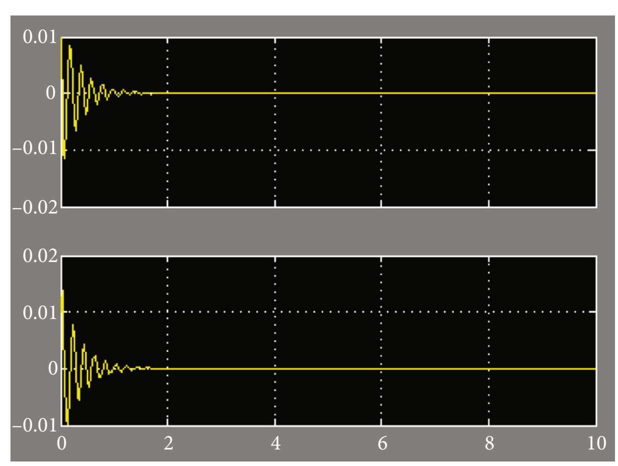

FIGURE 30: The simulation result using optimal control $G_{\alpha_3}(s)$. Initial condition: $x_1 = 0.01$, $x_2 = 0.01$.

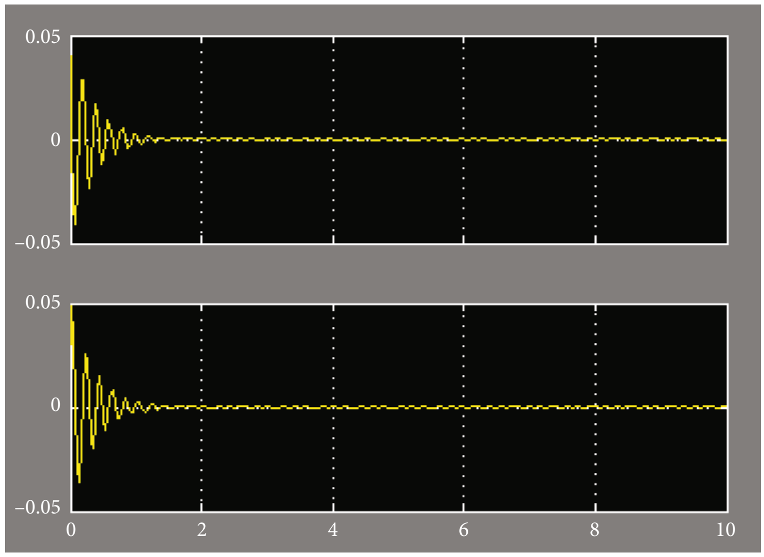

Figure 31: The simulation result using optimal control $G_{\alpha_3}(s)$. Initial condition: $x_1 = 0.04$, $x_2 = 0.03$.

The author calculate the value of the matrix K_{α_2} through Matlab software:

$$K_{\alpha_2} = lqr\left(A_{\alpha_2}, B_{\alpha_2}, Q_{\alpha_2}, R_{\alpha_2}\right)$$
$$G_{\alpha_3}(s) = \frac{-479.8}{s^2 + 965.3}$$
$$A_{\alpha_3} = \begin{bmatrix} 0 & -30.17 \\ 32 & 0 \end{bmatrix}; B_{\alpha_3} = \begin{bmatrix} 4 \\ 0 \end{bmatrix}; C_{\alpha_3} = \begin{bmatrix} 0 & -3.748 \end{bmatrix} \quad (35)$$

The author consider the system to have the external impact $(u \neq 0)$:

$$\dot{x} = A_{\alpha_3} x + B_{\alpha_3} u \quad (36)$$

The author need to find the matrix K_{α_3} of the optimal control vector: $u(t) = -K_{\alpha_3} * x(t)$ satisfy the quality index value of J_{α_3} and J_{α_3} must reach the minimum value:

$$J_{\alpha_3} = \int_0^{\infty} \left(x^T Q_{\alpha_3} x + u^T R_{\alpha_3} u\right) dt \quad (37)$$

where Q_{α_3} is a positive deterministic matrix, R_{α_3} is a positive deterministic matrix.

The matrix of K_{α_3} is determined from Riccati's equation of the form:

$$K_{\alpha_3} = R_{\alpha_3}{}^{-1} B_{\alpha_3}{}^{T} P \quad (38)$$

The state feedback control structure is shown below (Figure 10).

Thus, the optimal control law for an optimal control problem with the quality criteria is a linear equation and it has the form:

$$u(t) = -K_{\alpha_3}(t) = -R_{\alpha_3}{}^{-1} B_{\alpha_3}{}^{T} P x(t) \quad (39)$$

The value of the matrix is P, P must be satisfied the equation:

$$P A_{\alpha_3} + A_{\alpha_3}{}^{T} P + Q_{\alpha_3} - P B_{\alpha_3} R_{\alpha_3}{}^{-1} B_{\alpha_3}{}^{T} P = \dot{P} \quad (40)$$

The equation (40) is known as Riccati's equation.

I choose the values of the matrix Q_{α_3} and the values of the matrix R_{α_3} as follows:

$$Q_{\alpha_3} = \begin{bmatrix} 1 & 0 \\ 0 & 1 \end{bmatrix}; R_{\alpha_3} = 1. \quad (41)$$

Then I calculate the value of the matrix K_{α_3} through Matlab software:

$$K_{\alpha_3} = lqr\left(A_{\alpha_3}, B_{\alpha_3}, Q_{\alpha_3}, R_{\alpha_3}\right) = \begin{bmatrix} 1.4339 & 0.066 \end{bmatrix}$$
$$G_{\alpha_4}(s) = \frac{479.8s^2 + 5.966 \times 10^{-12} s + 1.639 \times 10^5}{s^4 + 965.3s^2}$$
$$A_{\alpha_4} = \begin{bmatrix} 0 & -30.17 & 0 & 0 \\ 32 & 0 & 0 & 0 \\ 0 & 1 & 0 & 0 \\ 0 & 0 & 1 & 0 \end{bmatrix}; B_{\alpha_4} = \begin{bmatrix} 64 \\ 0 \\ 0 \\ 0 \end{bmatrix};$$
$$C_{\alpha_4} = \begin{bmatrix} 0 & 0.2343 & 2.913 \times 10^{-15} & 80.03 \end{bmatrix} \quad (42)$$

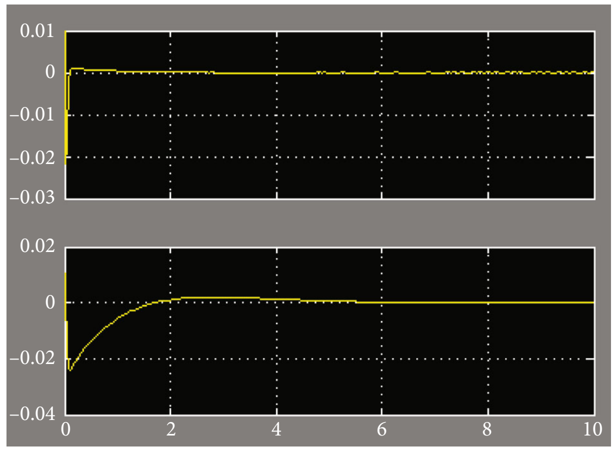

FIGURE 32: The simulation result using optimal control $G_{\alpha_4}(s), G_{\alpha_2}(s)$. Initial condition: $x_1 = 0.01$, $x_2 = 0.01$, $x_3 = 0.01$, $x_4 = 0.01$.

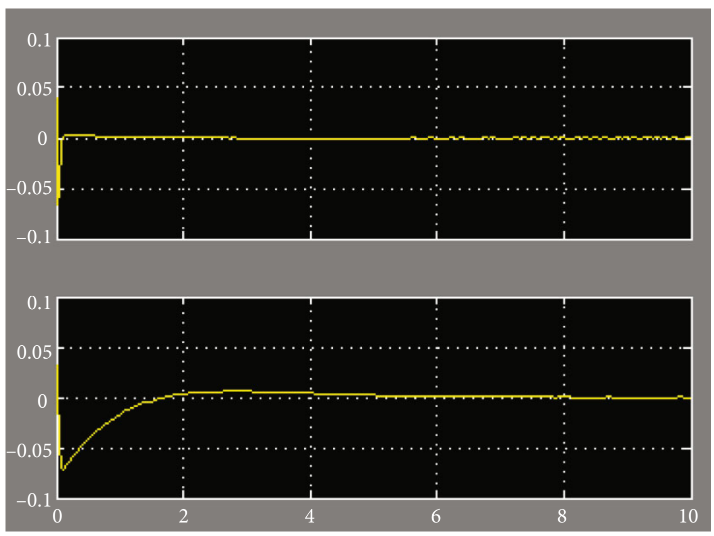

FIGURE 33: The simulation result using optimal control $G_{\alpha_4}(s), G_{\alpha_2}(s)$. Initial condition: $x_1 = 0.04$, $x_2 = 0.03$, $x_3 = 0.03$, $x_4 = 0.03$.

I consider the system to have the external impact $(u \neq 0)$:

$$\dot{x} = A_{\alpha_4} x + B_{\alpha_4} u \tag{43}$$

I need to find the matrix K_{α_4} of the optimal control vector: $u(t) = -K_{\alpha_4} * x(t)$ satisfy the quality index value of J_{α_4} and J_{α_4} must reach the minimum value:

$$J_{\alpha_4} = \int_0^{\infty} \left(x^T Q_{\alpha_4} x + u^T R_{\alpha_4} u\right) dt \tag{44}$$

where Q_{α_4} is a positive deterministic matrix, R_{α_4} is a positive deterministic matrix.

The matrix of K_{α_4} is determined from Riccati's equation of the form:

$$K_{\alpha_4} = R_{\alpha_4}{}^{-1} B_{\alpha_4}{}^{T} P \tag{45}$$

The state feedback control structure is shown below (Figure 11).

Thus, the optimal control law for an optimal control problem with the quality criteria is a linear equation and it has the form:

$$u(t) = -K_{\alpha_4}(t) = -R_{\alpha_4}{}^{-1} B_{\alpha_4}{}^{T} P x(t) \tag{46}$$

The value of the matrix is P, P must be satisfied the equation:

$$P A_{\alpha_4} + A_{\alpha_4}{}^{T} P + Q_{\alpha_4} - P B_{\alpha_4} R_{\alpha_4}{}^{-1} B_{\alpha_4}{}^{T} P = \dot{P} \tag{47}$$

The equation (47) is known as Riccati's equation.

I choose the values of the matrix Q_{α_4} and the values of the matrix R_{α_4} as follows:

$$Q_{\alpha_4} = \begin{bmatrix} 1 & 0 & 0 & 0 \\ 0 & 1 & 0 & 0 \\ 0 & 0 & 1 & 0 \\ 0 & 0 & 0 & 1 \end{bmatrix}, R_{\alpha_4} = 1. \tag{48}$$

Then I calculate the value of the matrix K_{α_4} through Matlab software:

$$K_{\alpha_4} = lqr\left(A_{\alpha_4}, B_{\alpha_4}, Q_{\alpha_4}, R_{\alpha_4}\right) = \left[1.3035 \quad 0.6991 \quad 1.8279 \quad 1.0000\right] \tag{49}$$

Figures 12, 13, 14, 15, 16, 17, 18, 19, 20, 21, 22 are shown below.

4. Simulation Results and Discussions

Simulation results are shown Figures 23, 24, 25, 26, 27, 28, 29, 30, 31, 32, 33.

My comments:

Figures 23, 24, 25, 26, 27 show that the amplitude of oscillation is large.

From Figures 28, 29, 30, 31, 32, 33 of the simulation results show me with the optimal controller, it will help stabilize the output signal of the system. However, if the input signal is large (Figures 28, 31, 33), then the oscillation range of the signal amplitude at the output is high before it is stabilized. The result in Figures 29, 30, 32 is better than in Figures 28, 31, 33. The simulation results accurately reflect the problem: the optimal controller performs better when there is no external force applied to the system, for example: noise levels of other signals ..The optimal controller used in this case is more efficient than the simulation result without using any algorithms.

From Figures 28, 29 and Figures 32, 33 it is shown that the system with 2 input pairs has slightly higher amplitude of oscillation than the system with one input pair in using the same controller. This shows that the more complex the system, the larger the amplitude of the vibration compared to the simple structure. Furthermore, this system with complex structure takes faster to return to steady state (2 sec) this the system with simpler structure (4 sec).

5. Conclusions

In this paper, it is proposed to investigate the operation of a flexible link system with 2 input pairs based on the simulation results to help the system achieve the desired functions. Besides, the simulation helps me to determine the values of the parameters to have the basis to control the operation of the system to suit the requirements. This also shows the flexibility in adjusting the parameters of modern controllers as it is applied to the above model. Through this survey, the research achievements on modern control theory for systems with relatively complex structure like the above system will be applied in the future. This method is useful for checking the operational status of all the existing components in a system. In the case of possible problems such as a failure of elements inside a server, this survey is a reference for quality control as well as the functions of these elements. For complex structured systems, the author can use control methods for each of the transfer functions in the host system. From there, the author took insight into the problem and the author was able to evaluate the host system's properties most accurately. In the future, the author can apply modern control algorithms like neural control in above model. Specifically, a neural control method is applied: a model with 1 input pair, a model with 2 input pairs...After that, the author evaluate the effect of the neural network for the above models. With the above controller applied in this paper, its efficiency has been tested for most of the subsystems in a system. This article is a premise for me to study for other complex models based on the above implemented contents. Another advantage of using the above controller for this model is that the time to steady state for the system is faster for the complex structures (2 input pairs) than for the simpler structure (1 input pair). The time to return to steady state is negligible (~0.1 sec -2 sec) for a system with 2 input pairs. This rarely happens for a system with a complex structure.

Data Availability

Readers are free to access supporting data for research conclusions from the references at the end of my paper.

Conflicts of Interest

The author(s) declare(s) that they have no conflicts of interest.

References

[1] A. Cristofaro, A. De Luca, and L. Lanari, "Linear-quadratic optimal boundary control of a one-link flexible arm," *IEEE Control Systems Letters*, vol. 5, no. 3, pp. 833–838, 2021.

[2] J. Liu and W. He, *Distributed Parameter Modeling and Boundary Control of Flexible Manipulators*, Springer, 2018.

[3] F. Bellezza, L. Lanari, and G. Ulivi, "Exact modeling of the flexible slewing link," in *Proceedings., IEEE International Conference on Robotics and Automation*, pp. 734–739, Cincinnati, OH, USA, May 1990.

[4] H. Kanoh, "Distributed parameter models of flexible robot arms," *Advanced Robotics*, vol. 5, no. 1, pp. 87–99, 1990.

[5] J.-H. Park and H. Asada, "Design and control of minimum-phase flexible arms with torque transmission mechanisms," in *Proceedings., IEEE International Conference on Robotics and Automation*, pp. 1790–1795, Cincinnati, OH, USA, May 1990.

[6] Y. Chang, S. Zhang, N. D. Alotaibi, and A. F. Alkhateeb, "Observer-Based Adaptive Finite-Time Tracking Control for a Class of Switched Nonlinear Systems With Unmodeled Dynamics," *IEEE Access*, vol. 8, pp. 204782–204790, 2020.

[7] Y. Wang, N. Xu, Y. Liu, and X. Zhao, "Adaptive fault-tolerant control for switched nonlinear systems based on command filter technique," *Applied Mathematics and Computation*, vol. 392, article 125725, 2021.

[8] X. Z. Jin, G. H. Yang, X. H. Chang, and W. W. Che, "Robust Fault-tolerant H∞ Control with Adaptive Compensation," *Acta Automatica Sinica*, vol. 39, no. 1, pp. 31–42, 2013.

[9] Y. Wang, B. Niu, H. Wang, N. Alotaibi, and E. Abozinadah, "Neural network-based adaptive tracking control for switched nonlinear systems with prescribed performance: An average dwell time switching approach," *Neurocomputing*, vol. 435, pp. 295–306, 2021.

[10] M. H. Korayem, H. Rahimi, and A. Nikoobin, "Path planning of Mobile elastic robotic arms by indirect approach of optimal control," *Journal of Advanced Robotic Systems*, vol. 8, no. 1, pp. 10–20, 2011.

[11] A. M. Shafei and M. H. Korayem, "Theoretical and experimental study of dynamic load-carrying capacity for flexible robotic arms in point-to-point motion," *Optimal Control, Applications and Methods*, vol. 38, no. 6, pp. 963–972, 2017.

[12] M. H. Korayem, A. M. Shafei, and S. F. Dehkordi, "Systematic modeling of a chain of N-flexible link manipulators connected by revolute-prismatic joints using recursive Gibbs-Appell formulation," *Archive of Applied Mechanics*, vol. 84, no. 2, pp. 187–206, 2014.

[13] M. H. Korayem, M. Irani, and S. Rafee Nekoo, "Load maximization of flexible joint mechanical manipulator using nonlinear optimal controller," *Acta Astronautica*, vol. 69, no. 7-8, pp. 458–469, 2011.

[14] QUANSER, *Rotary Flexible Link*, Workbook, 2011.

[15] Y.-G. Tang, F. C. Sun, Z. Q. Sun, and T. L. Hu, "Tip position control of a flexible link manipulator with neural networks," *International Journal of Control Automation and System*, vol. 4, no. 3, pp. 308–317, 2006.